Strongly perturbed state-selective charge exchange between slow Ar^{8+} and He

R. T. Zhang [1,4,*,†] J. W. Gao [2,*,‡] Y. W. Zhang,[5] D. L. Guo,[1,4] Y. Gao,[1,4] X. L. Zhu [1,4] J. W. Xu,[1] D. M. Zhao,[1] S. Yan,[1,4] S. Xu,[1,4] S. F. Zhang,[1,4] Y. Wu,[3,5] J. G. Wang,[3] and X. Ma [1,4,§]

[1]*Institute of Modern Physics, Chinese Academy of Sciences, Lanzhou 730000, People's Republic of China*
[2]*School of Physics, Hangzhou Normal University, Hangzhou 311121, People's Republic of China*
[3]*Key Laboratory of Computational Physics, Institute of Applied Physics and Computational Mathematics,*
Beijing 100088, People's Republic of China
[4]*University of Chinese Academy of Sciences, Beijing 100049, People's Republic of China*
[5]*HEDPS, Center of Applied Physics and Technology, Peking University, 100871 Beijing, People's Republic of China*

We report an experimental and theoretical study of state-selective charge exchange processes in Ar^{8+} on He collisions at 1 and 3 keV/amu, benchmarking the fundamental electron capture dynamics under strong perturbations. The quantum-state selectivity has been experimentally resolved for one $1s$ electron of He capture into $4s$, $4p$, $4d + 4f$, and $5s$ states of Ar^{7+} ion along with the corresponding scattering angle differential cross sections. By comparing to theoretical calculations with a two-active-electron semiclassical asymptotic-state close-coupling approach, we are able to verify the important role of electronic correlations during the collisions and that the impact parameter sensitive transition probability significantly mediates the state-selective specifics.

The reaction of charge exchange (CX) between highly charged ions (HCIs) and neutrals is a fundamental process of dynamical two-center quantum state transition. It has been the subject of intensive theoretical and experimental studies, motivated by understanding of few-body problems [1,2], and diagnosing of fusion and astrophysical plasmas [3–7]. Differing from CX at high energy collisions, a simple velocity matching and impulsive approximation are no longer valid owing to the nonadiabaticity at low collision energies [8–14]. For simplicity, a single-active-electron treatment with an independent-particle model has long been used for CX involving few- or many-electron targets [15], despite its insufficient accuracy in describing experimental observations [16]. In particular, the low-energy HCIs conditions strongly perturb electron transition, which even stresses the challenging towards understanding CX dynamics.

With the advent of advanced experimental techniques, the details of $n\ell$-resolved state-selective capture can be unraveled for slow HCIs (n and ℓ are principal quantum number and orbital angular momentum number, respectively). Using a high-resolution x-ray spectrometer, Leutenegger *et al.* [17] have measured emissions following CX between Ar^{18+} and P^{15+}, and H$_2$, and found high end Lyman series is greater by

a factor of two for P^{14+} than for Ar^{17+}. Another significant development is the cold target recoil ion momentum spectroscopy (COLTRIMS) [18,19], with which state-selective and the scattering angle differential cross sections can be solely obtained [20–22]. Otranto *et al.* [23] have attributed the oscillatory structure of the transverse momentum distribution in 1–10 keV/amu Ne^{8+} CX with Na($3s$) to electron swaps by comparing to classical trajectory Monte Carlo calculations. A Fraunhofer-type diffraction has been revealed for n- and ℓ-resolved state-selective capture in C^{4+} on He collisions [24], which extends the previous study of Van der Poel *et al.* [25]. Consequently, the unexplored structures in the transition probabilities could become feasible experimentally for the scattering angle of the projectile.

In this paper, we investigate the collision dynamics of Ar^{8+} single CX with He at 1 keV/amu and 3 keV/amu, where the strong perturbations with strengths are $v_e/v_p = 3.8$, 6.7 (v_e and v_p are the classical 1s orbital velocity of He and the projectile velocity, respectively). Although previous studies show that cross sections of $n = 4$ capture are predominant for the collision energy from 20 eV/amu to 25 keV/amu (the perturbation strengths are from 2.7 to 47.6) [26–28], scattering angle differential cross sections are sparsely reported. The present $n\ell$-resolved single CX state-selectivity and the corresponding scattering angle differential ones are measured using the COLTRIMS setup and compared with theoretical results calculated with a two-active-electron semiclassical asymptotic-state close-coupling (SCASCC) approach, which succeeds in quantitatively reproducing total cross sections for various CX processes [29–32]. Our state-of-the-art calculations give an excellent description of the present measured state-selective CX cross sections in both magnitude and shape. Thereby, we make an essential step in the understanding of CX dynamics with two active electrons under strong perturbations.

---

*These authors contributed equally to this work.

†zhangrt@impcas.ac.cn
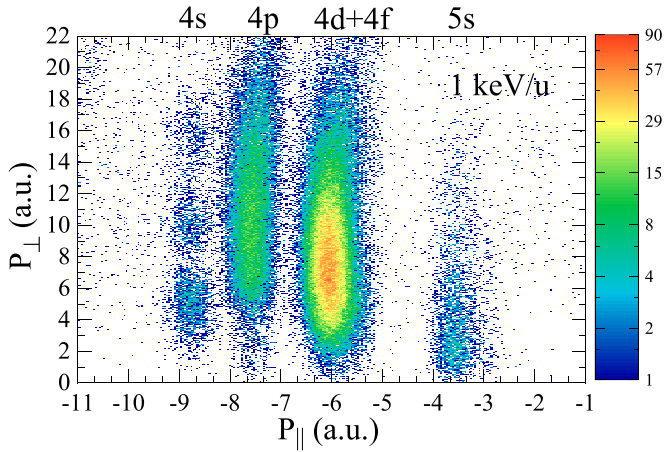‡gaojunwen@hznu.edu.cn
§x.ma@impcas.ac.cn

FIG. 1. Two-dimensional momentum distributions in the 1 keV/amu Ar^{8+} CX with He. The horizontal axis and the vertical axis represent the longitudinal recoil ion momentum $P_{||}$ and the transversal recoil ion momentum $P_{\perp}$, respectively.

The experiment was carried out with the COLTRIMS setup at the low energy electron beam ion source (EBIS) laboratory in the Institute of Modern Physics, Chinese Academy of Sciences. The experimental setup used here is basically the same as described in previous publications [22,33]. In brief, a beam of Ar^{8+} ions from the EBIS source intersected with a supersonic He gasjet in the center of a time-of-flight (TOF) spectrometer. Lengths of the accelerating tube and the drifting tube of the TOF spectrometer were 107.5 and 215 mm, respectively. This arrangement meets the Wiley-McLaren time focusing condition [34]. The recoil ions He^+ and He^{2+} were extracted by a homogeneous electric field of 8.3 V/cm and detected by a position and time sensitive detector (PSD). The charge changed projectile ions Ar^{7+} and Ar^{6+} were separated from the primary Ar^{8+} ion beam by an electrostatic deflector downstream of the collision chamber and detected by another PSD. With the measured TOF and position information of recoil ions, the longitudinal and transversal momentum of recoil ions were reconstructed [22], as illustrated in Fig. 1. The longitudinal recoil ion momentum $P_{||}$ and the transversal recoil ion momentum $P_{\perp}$ reflect the state-selectivity and scattering angle differential cross sections, respectively. Atomic units (a.u.) are used throughout this paper unless otherwise stated.

Theoretically, the SCASCC method has been previously described in, e.g., [29–31,35,36]. The theoretical treatment is semiclassical in that the relative target-projectile motion is described by classical straight-line trajectory with constant velocity, while the electronic dynamics is treated quantum mechanically, by nonperturbatively solving the time-dependent Schrödinger equation (TDSE) for a two-electron Hamiltonian, including the Coulombic interactions between all particles. In the present calculations, the two electrons on the He target are treated as active electrons, while the Ar^{8+} ion is described with the frozen-core electron approximation in which the inner-shell electrons are assumed to be inactive. The interaction of these frozen electrons and the nucleus with the two active ones is described by the model potential [31]. To describe the He^+, He, Ar^{7+}, and Ar^{6+} electronic states,

we use the same Gaussian-type orbital (GTO) sets as in [31] from which spin-adapted products are constructed to diagonalize the isolated target and projectile Hamiltonians within a full configuration interaction formalism. The TDSE then reduces to a set of coupled differential equations for the time-dependent coefficients, which asymptotically are the probability amplitudes from which integral (total) cross sections are evaluated. In the same manner as in [24,37], the scattering angle differential cross sections for inelastic processes are expressed in the center of mass frame as

$$
\begin{aligned}
\frac{d\sigma_{fi}}{d\Omega} &= |f_{fi}(\theta, \phi)|^2 \\
&= |\mu v(-i)^{1+|\Delta m_{fi}|} e^{-i\Delta m_{fi}\phi} \\
&\quad \times \int_0^\infty b\,db\,J_{|\Delta m_{fi}|}(2\mu v b \sin(\theta/2))c_f(b, v_P)|^2, \quad (1)
\end{aligned}
$$

where the scattering amplitude f_{fi} is given as a Bessel transform of the collision amplitude $c_f(b, v_P)$, μ is the reduced mass of the target and projectile, $\Delta m_{fi} = m_f - m_i$ with m_i, m_f the magnetic quantum numbers of the initial and final states, respectively. It should be noted that all b-dependent phases (i.e., common phases due to the core-core interaction in the Hamiltonian [38]) should be included in the collision amplitudes $c_f(b, v_P)$ of Eq. (1). It is precisely the complete phase information that allows the extraction of the angular predictions from straight-line trajectory collision amplitudes. Explicitly, the amplitudes are

$$
c_f(b, v_P) = a_f(b, v_P) \exp\left(\frac{i}{v_P} 2Z^T Z^P \ln b\right), \quad (2)
$$

where Z^T and Z^P are, respectively, the target and projectile charges, the amplitude $a_f(b, v_P)$ is obtained by solving the coupled differential equations reduced from TDSE in a large, but finite, time domain.

The calculations presented in this work include 5982 singlet states and pseudostates in total, describing elastic, single CX, double CX, and ionization channels. The convergence for 4ℓ-resolved CX cross sections was evaluated to be better than 15% [31].

Figure 1 shows the measured recoil ion momentum distribution at the collision energy of 1 keV/amu, where $n = 4$ capture is predominant. This agrees with the extrapolation from a recent measurement [39] and the prediction by $q^{3/4}/\sqrt{I_n/13.6}$ [40,41], where I_n is the ionzation energy of a neutral target and 24.6 eV for He. For the $n = 4$ capture, state-selective populations are distinguished for electron capture into $4s$, $4p$, and $4d + 4f$ states. Note that the experimental resolution is not adequate to discern $4d$ and $4f$ capture processes. For $n = 5$ capture, only $5s$ capture is observed. In addition, it is inferred that there is a large energy level gap between $n = 3$ capture and the initial channel for the present CX process, this results in a negligible contribution of $n = 3$ capture [27,39].

Our measured and calculated relative state-selective CX cross sections for Ar^{8+} and He collisions at 1 keV/amu are presented in Table I, as well as available experimental and theoretical results. The present experimentally derived fractions for $4s$, $4p$, $4d + 4f$, and $5s$ capture are 3.5%, 22.5%, 70.7%, and 3.3%, respectively, which agree with previous

TABLE I. Relative state-selective capture cross sections for CX between Ar^{8+} and He at 1 keV/amu. Gaussian fittings are used by minimizing the reduced χ^2 value of the composite fitting in all spectra. The statistical errors are less than 0.5%.

nl	Ours(%)		Other results (%)			
	Expt.	SCASCC	a	b	c	d
$4s$	3.5	3.6	3.7	5	4	7.2
$4p$	22.5	22.6	23.0	29	21	35.6
$4d + 4f$	70.7	70.4	71.2	66	75	52.4
$5s$	3.3	3.5	3.1			3

a: experiment [28]; b: experiment (error $\pm 30\%$) [27];
c: perturbation theory [27]; d: coupled channel theory [28].

measurements [27,28]. The SCASCC calculations are in better agreement with the measurements, compared to the results from the previous perturbation theory [27] and single-active-electron coupled-channel method [28]. Similar conclusions at 6.25 and 25 keV/amu can be seen in a very recent publication [31].

Figure 2 presents the comparison of state-selective single CX scattering angle distributions between the SCASCC cal-

culations and present measurements at 1 keV/amu, as well as the previous experimental and theoretical results from [22] at 3 keV/amu. It can be observed that the scattering angle θ_{LAB} extends to 2.0 mrad at 1 keV/amu, while it is only within 0.6 mrad at 3 keV/amu. This can be qualitatively explained due to a longer interaction time at 1 keV/amu, which results in a larger scattering angle. Note that for the 3 keV/amu impact energy the two-center atomic orbital close coupling (TC-AOCC) calculations from [22], which is a single-active-electron treatment, show considerable deviations from the measurement. As pointed out in [22], such deviations are probably caused by not considering electron correlations therein. Here, we take into account explicitly electron-electron correlation and electron exchange effects between two active electrons. By normalizing the measured results to the present calculated scattering angle differential cross sections, the SCASCC results agree well with the measurements for $1s$ to $4s$, $4p$, and $4d + 4f$ capture for both 1 and 3 keV/amu. Thus, we clarify that electronic correlations play an important role in the present collision system at low energies, and cannot be neglected.

Apparently oscillatory structures with three clear lobes and a weak one at large angle, and with two clear lobes are observed in the scattering angle differential cross sections for $1s$
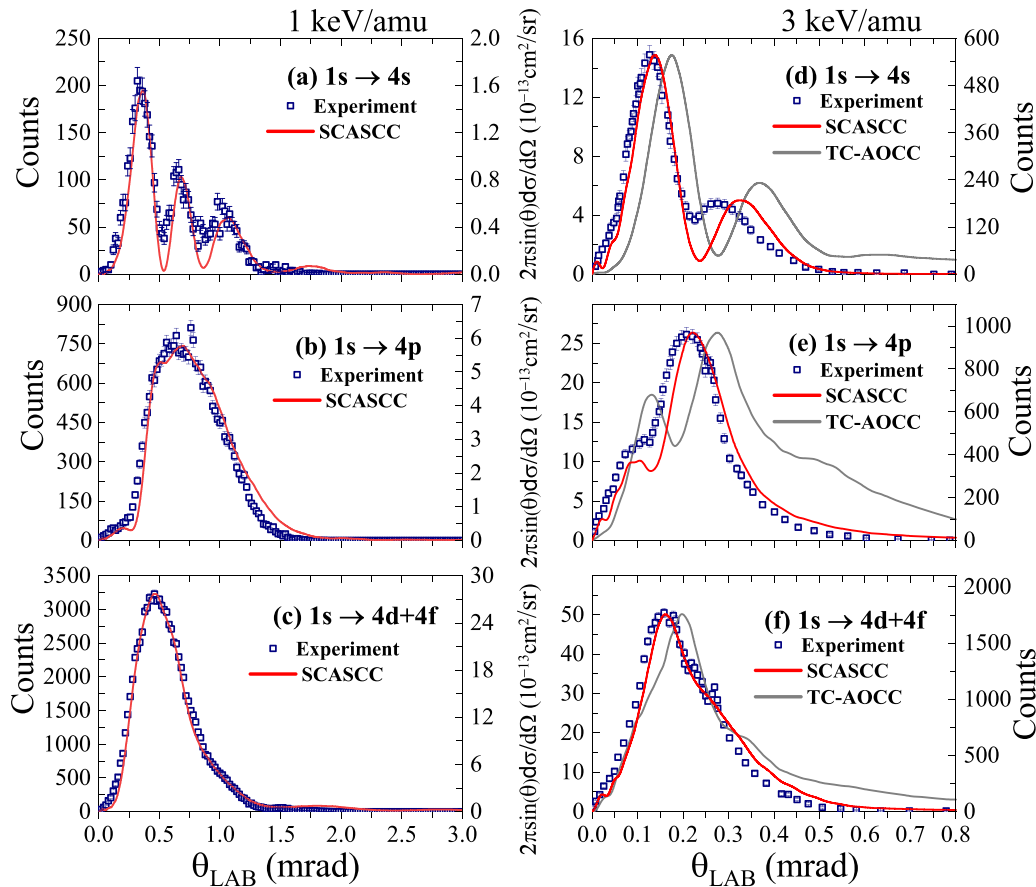

FIG. 2. Differential cross sections for capture into $4s$, $4p$, and $4d + 4f$ states as a function of θ_{LAB}, scattering angle in the laboratory frame, for Ar^{8+} CX with He. The open squares and solid lines represent the measurements and calculations, respectively. Panels (a), (b), and (c) represent the comparison between the experimental results and SCASCC calculations at 1 keV/amu; Panels (d), (e), and (f) represent the comparison among SCASCC, TC-AOCC, and experimental results at 3 keV/amu. The measured results and TC-AOCC calculations for 3 keV/amu are also seen in Ref. [22].
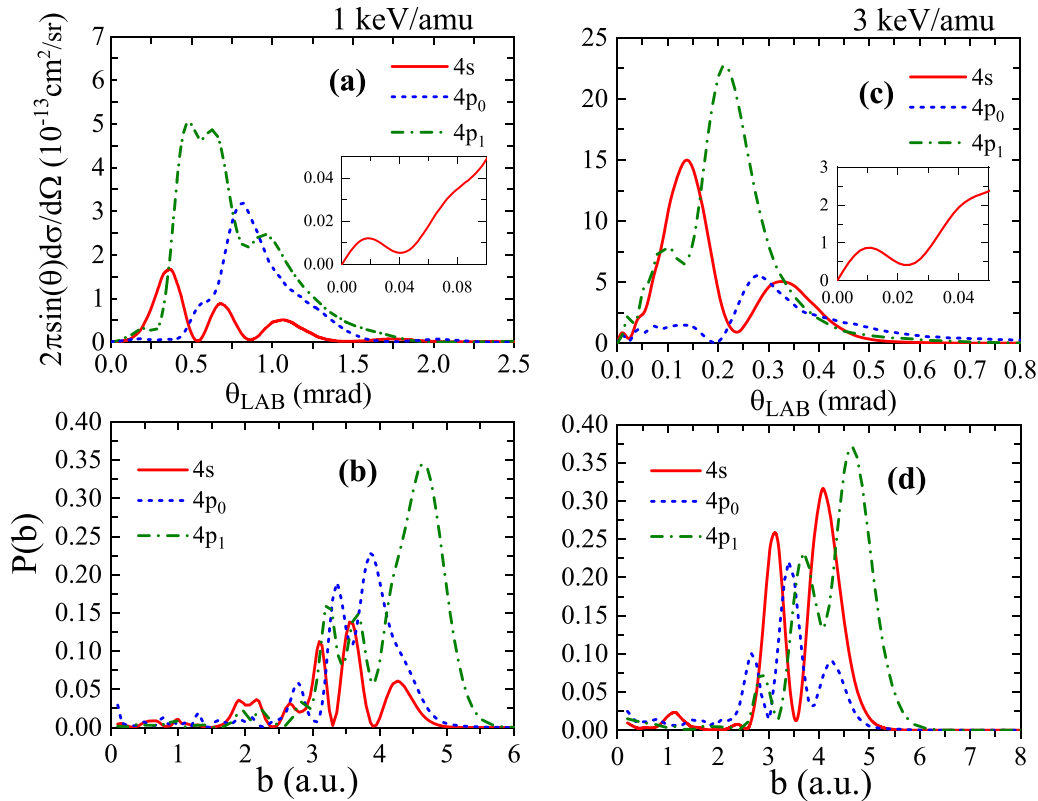
FIG. 3. (a), (c) Our calculated scattering angle differential cross sections for single electron capture into Ar^{7+} ($4s$, $4p_0$, and $4p_1$) as a functions of scattering angle; (b), (d) The transition probabilities for electron capture into Ar^{7+} ($4s$, $4p_0$, and $4p_1$) as a function of impact parameter b.

to $4s$ capture at 1 keV/amu and 3 keV/amu, respectively. Similar structures observed in scattering angle differential cross sections were interpreted by the Fraunhofer-type diffraction (see Refs. [24,25,42–44] and references therein), where the first minimum in the cross sections is located at $0.61\lambda/\rho$, ρ is the aperture radius, and λ the wavelength of incident matter wave. In the present study, at 1 keV/amu, the *de Broglie* wavelength of the projectile ion Ar^{8+} is 4.31×10^{-4} a.u. in the laboratory frame. The aperture radius can be estimated from the maximum of the effective impact parameter, $\rho = 5.0$ a.u. as shown in Fig. 3(b). Thus, one can compute the position of the first minimum, which is about $\theta_{LAB} = 0.05$ mrad. Indeed, one can observe a minimum in the scattering angle differential cross section for $1s$ to $4s$ capture located around 0.05 mrad in the inset of Fig. 3(a). However, the present scattering angle θ_{LAB} extends to 2.0 mrad. This clarifies that the contribution of the Fraunhofer-type diffraction to the dominant oscillatory structures is negligible in the present capture process. At 3 keV/amu, the estimated minimum resulting from Fraunhofer-type diffraction is located around 0.027 mrad, and in agreement with the one shown in the inset of Fig. 3(c), which is also negligible compared to the dominant oscillatory structures.

To get further insight into the oscillatory structures, we present in Fig. 3 the calculated scattering angle differential cross sections for electron capture into $4s$, $4p_0$, and $4p_1$ (the subscript of magnetic quantum number 1 in $4p_1$ is the absolute value of ± 1 in $4p_{\pm 1}$ unless it is stated otherwise), together with corresponding impact-parameter-dependent transition

probabilities at 1 and 3 keV/amu. Note that, in the SCASCC method, Cartesian GTOs are used where p_0 orbital orients along the z-axis, and p_1 orbital orients along the x axis (see collision geometry in Fig. 1 of [31]). In Fig. 3(b) transition probabilities for $4s$ capture process at 1 keV/amu are dominated by three strong peaks at large impact parameter b at 3–5 a.u., and several weak ones at smaller b. In general, small-angle scattering implies the dominant contribution of distant trajectories (large b), and vice versa. A comparison between transition probabilities and scattering angle differential cross sections may suggest that oscillatory structures with three clear lobes shown in Fig. 3(a) are correlated with the three strong peaks in Fig. 3(b), and the weak lobe at the larger angle is correlated with the weak peaks in the smaller b transition probabilities. At 3 keV/amu, the cross section for $4s$ capture process in Fig. 3(c) show two clear lobes, and the corresponding transition probabilities are also dominated by two strong peaks for b at 2–5 a.u..

Furthermore, the relative contributions of the magnetic substates are investigated by considering dynamical couplings at strong perturbations [45–47]. First, the SCASCC calculations show that the scattering angle differential cross sections for the $4p_1$ capture is dominant over the $4p_0$ one; this is in accordance with propensity rules [48–51]. That is, the projectile ions transferring the angular momentum leads to that electron orbital angular momentum mainly orients perpendicular to the scattering plane, which is defined by the projectile ion moving vector and internuclear vector between two collision partners. Second, the oscillatory structures in the

cross sections of $4s$, $4p_0$, and $4p_1$ behave in a similar way with the corresponding transition probabilities for both 1 and 3 keV/amu. For example, in the transition probabilities at 1 keV/amu shown in Fig. 3(b), the $4s$ oscillations are similar with the $4p_1$ ones (except a slight shift toward small b) but in opposite phases with the $4p_0$ ones. In Fig. 3(a), the cross sections for electron capture into $4s$ and $4p_1$ also show similar oscillations but with opposite phases compared to $4p_0$ ones. At 3 keV/amu, in Figs. 3(c) and 3(d) the $4s$ oscillations are close to the $4p_0$ ones but in opposite phases with $4p_1$ ones. These suggest that the impact-parameter sensitive transition probabilities mediate the oscillatory structures in the scattering angle differential cross sections. Moreover, the transition probabilities are essentially determined by the collision energy dependent couplings among electron capture into $4s$, $4p_0$, and $4p_1$.

In conclusion, we present a joint experimental and theoretical study of CX between 1–3 keV/amu Ar^{8+} and He with COLTRIMS, with the strong perturbation strengths of 3.8 and 6.7, respectively. The state-selectivity of CX has been resolved for one $1s$ electron of He capture into $4s$, $4p$, $4d + 4f$, and $5s$ states of Ar^{7+} ion. Our SCASCC calculations, taking into account both electronic correlations between the two active electrons and important one- and two-electron channels, reproduce well the measured state-selective capture

cross sections and the scattering angle differential ones. Comparison with the existing theoretical calculations demonstrates the importance of the electronic correlation effects. We also find the correspondence of oscillatory structures between the scattering angle differential cross sections and the impact parameter dependent transition probabilities. To this end, we are able to conclude that the impact parameter sensitive transition probability significantly mediates the state-selective capture specifics. This study possibly extends CX studies now into a regime of highly excited quantum-state selective dynamics associated with electron orbital angular momentum orientation at stronger perturbations.

[1] B. H. Bransden and M. R. C. McDowell, *Charge Exchange and the Theory of Ion-Atom Collisions* (Oxford University Press, New York, 1992).

[2] J. Ullrich and V. Shevelko, *Many-Particle Quantum Dynamics in Atomic and Molecular Fragmentation* (Springer Berlin, Heidelberg, 2003).

[3] J. E. Rice, E. S. Marmar, J. L. Terry, E. Kallne, and J. Kallne, Observation of Charge-Transfer Population of High-n Levels in Ar^{16+} from Neutral Hydrogen in the Ground and Excited States in a Tokamak Plasma, Phys. Rev. Lett. **56**, 50 (1986).

[4] R. C. Isler, Observation of the Reaction $H^0 + O^{8+} \rightarrow H^+(O^{7+})$ During Neutral-Beam Injection into Ormak, Phys. Rev. Lett. **38**, 1359 (1977).

[5] H. Folkerts, F. Bliek, L. Meng, R. Olson, R. Morgenstern, M. von Hellermann, H. Summers, and R. Hoekstra, He^{2+}- He collisions: One-electron capture and target-ion excitation, J. Phys. B: At. Mol. Opt. Phys. **27**, 3475 (1994).

[6] T. E. Cravens, Comet hyakutake x-ray source: Charge transfer of solar wind heavy ions, Geophys. Res. Lett. **24**, 105 (1997).

[7] P. Beiersdorfer, K. R. Boyce, G. V. Brown, H. Chen, S. M. Kahn, R. L. Kelley, M. May, R. E. Olson, F. S. Porter, C. K. Stahle, and W. A. Tillotson, Laboratory simulation of charge exchange-produced X-ray emission from comets, Science **300**, 1558 (2003).

[8] E. C. G. Stückelberg, Theory of inelastic collisions between atoms, Helv. Phys. Acta **5**, 369 (1932).

[9] D. Dijkkamp, D. Ciric, E. Vileg, A. de Boer, and F. J. de Heer, Subshell-selective electron capture in collisions of C^{4+}, N^{5+}, O^{6+} with H, H_2 and He, J. Phys. B: At. Mol. Opt. Phys. **18**, 4763 (1985).

[10] F. W. Bliek, G. R. Woestenenk, R. Hoekstra, and R. Morgenstern, State-selective electron-capture measurements for N^{4+}- H and N^{4+}- H_2 collisions, Phys. Rev. A **57**, 221 (1998).

[11] D. Voulot, D. R. Gillen, D. M. Kearns, R. W. McCullough, and H. B. Gilbody, State-selective one-electron capture by slow state-prepared $N^{2+}(2p)$ ground-state ions in collisions with hydrogen atoms, J. Phys. B: At. Mol. Opt. Phys. **34**, 1039 (2001).

[12] W. Lichten, Resonant charge exchange in atomic collisions, Phys. Rev. **131**, 229 (1963).

[13] D. R. Schultz, C. O. Reinhold, and P. S. Krstić, Analysis of Unexplained Oscillations in Intermediate-Energy Ion-Atom Collisions, Phys. Rev. Lett. **78**, 2720 (1997).

[14] J. Eichler, in *Lectures on Ion-Atom Collisions*, North-Holland Personal Library (Elsevier Science, Amsterdam, 2005) p. x.

[15] W. Fritsch and C. Lin, The semiclassical close-coupling description of atomic collisions: Recent developments and results, Phys. Rep. **202**, 1 (1991).

[16] F. Aumayr, K. Ueda, E. Sokell, S. Schippers, H. Sadeghpour, F. Merkt, T. F. Gallagher, F. B. Dunning, P. Scheier, O. Echt, T. Kirchner, S. Fritzsche, A. Surzhykov, X. Ma, R. Rivarola, O. Fojon, L. Tribedi, E. Lamour, J. R. C. López-Urrutia, Y. A. Litvinov, V. Shabaev, H. Cederquist, H. Zettergren, M. Schleberger, R. A. Wilhelm, T. Azuma, P. Boduch, H. T. Schmidt, and T. Stöhlker, Roadmap on photonic, electronic and atomic collision physics: III. heavy particles: With zero to relativistic speeds, J. Phys. B: At. Mol. Opt. Phys. **52**, 171003 (2019).

[17] M. A. Leutenegger, P. Beiersdorfer, G. V. Brown, R. L. Kelley, C. A. Kilbourne, and F. S. Porter, Measurement of Anomalously Strong emission from the $1s-9p$ Transition in the Spectrum of

H-like Phosphorus Following Charge Exchange with Molecular Hydrogen, Phys. Rev. Lett. **105**, 063201 (2010).

[18] R. Dörner, V. Mergel, O. Jagutzki, L. Spielberger, J. Ullrich, R. Moshammer, and H. Schmidt-Böcking, Cold target recoil ion momentum spectroscopy: A momentum microscope to view atomic collision dynamics, Phys. Rep. **330**, 95 (2000).

[19] J. Ullrich, R. Moshammer, A. Dorn, R. Dörner, L. P. H. Schmidt, and H. Schmidt-Böcking, Recoil-ion and electron momentum spectroscopy: Reaction-microscopes, Rep. Prog. Phys. **66**, 1463 (2003).

[20] D. Fisher, B. Feuerstein, R. D. DuBois, R. Moshammer, J. R. C. López-Urrutia, I. Draganic, H. Lórch, A. N. Perumal, and J. Ullrich, State-resolved measurements of single-electron capture in slow Ne^{7+}- and Ne^{8+}-helium collisions, J. Phys. B: At. Mol. Opt. Phys. **35**, 1369 (2002).

[21] A. Cassimi, S. Duponchel, X. Flechard, P. Jardin, P. Sortais, D. Hennecart, and R. E. Olson, State-Selective Electron Capture in Low Velocity Multiply Charged Ion, Helium Collisions, Phys. Rev. Lett. **76**, 3679 (1996).

[22] R. T. Zhang, X. L. Zhu, X. Y. Li, L. Liu, S. F. Zhang, W. T. Feng, D. L. Guo, Y. Gao, D. M. Zhao, J. G. Wang, and X. Ma, Single-electron capture in 3-keV/u Ar^{8+}- He collisions, Phys. Rev. A **95**, 042702 (2017).

[23] S. Otranto, I. Blank, R. E. Olson, and R. Hoekstra, Evidence of electron saddle swap oscillations in angular differential ion–atom charge exchange cross sections, J. Phys. B: At. Mol. Opt. Phys. **45**, 175201 (2012).

[24] D. L. Guo, J. W. Gao, S. F. Zhang, X. L. Zhu, Y. Gao, D. M. Zhao, R. T. Zhang, Y. Wu, J. G. Wang, A. Dubois, and X. Ma, State-selective single-electron capture in intermediate-energy C^{4+} + He collisions, Phys. Rev. A **103**, 032827 (2021).

[25] M. van der Poel, C. V. Nielsen, M.-A. Gearba, and N. Andersen, Fraunhofer Diffraction of Atomic Matter Waves: Electron Transfer Studies with a Laser Cooled Target, Phys. Rev. Lett. **87**, 123201 (2001).

[26] M. Kimura and R. E. Olson, Electron capture in pseudo-two-electron systems: Ar^{8+} + He, Phys. Rev. A **31**, 489 (1985).

[27] M. Druetta, S. Martin, T. Bouchama, C. Harel, and H. Jouin, Spectroscopic study of the charge-exchange collision between Ar^{8+} and He or H_2 at beam energies of 80, 40, and 8 keV, Phys. Rev. A **36**, 3071 (1987).

[28] M. A. Abdallah, W. Wolff, H. E. Wolf, E. Sidky, E. Y. Kamber, M. Stöckli, C. D. Lin, and C. L. Cocke, Cold-target recoil-ion-momentum spectroscopy study of single electron capture from He by slow Ar^{8+} ions, Phys. Rev. A **57**, 4373 (1998).

[29] N. Sisourat, I. Pilskog, and A. Dubois, Nonperturbative treatment of multielectron processes in ion-molecule scattering: Application to He^{2+}- H_2 collisions, Phys. Rev. A **84**, 052722 (2011).

[30] J. W. Gao, Y. Wu, J. G. Wang, A. Dubois, and N. Sisourat, Double Electron Capture in H^+ + H^- Collisions, Phys. Rev. Lett. **122**, 093402 (2019).

[31] Y. W. Zhang, J. W. Gao, Y. Wu, J. G. Wang, N. Sisourat, and A. Dubois, Single- and double-electron capture in intermediate-energy Ar^{8+} + He collisions, Phys. Rev. A **106**, 042809 (2022).

[32] X. Ma, S. Zhang, W. Wen, Z. Huang, Z. Hu, D. Guo, J. Gao, B. Najjari, S. Xu, S. Yan, K. Yao, R. Zhang, Y. Gao, and X. Zhu, Atomic structure and collision dynamics with highly charged ions, Chin. Phys. B **31**, 093401 (2022).

[33] J. W. Xu, C. X. Xu, R. T. Zhang, X. L. Zhu, W. T. Feng, L. Gu, G. Y. Liang, D. L. Guo, Y. Gao, D. M. Zhao, S. F. Zhang, M. G. Su, and X. Ma, Measurement of *n*-resolved state-selective charge exchange in $Ne^{8,9+}$ collision with He and H_2, Astrophys. J. Suppl. Series **253**, 13 (2021).

[34] W. C. Wiley and I. H. McLaren, Time-of-flight mass spectrometer with improved resolution, Rev. Sci. Instrum. **26**, 1150 (1955).

[35] J. W. Gao, Y. Wu, N. Sisourat, J. G. Wang, and A. Dubois, Single-and double-electron transfer in low-and intermediate-energy C^{4+} + He collisions, Phys. Rev. A **96**, 052703 (2017).

[36] Y. W. Zhang, J. W. Gao, Y. Wu, F. Y. Zhou, J. G. Wang, N. Sisourat, and A. Dubois, Single- and double-electron capture in intermediate-energy N^{5+} + H_2 collisions, Phys. Rev. A **102**, 022814 (2020).

[37] A. Dubois, S. E. Nielsen, and J. P. Hansen, State selectivity in H^+- Na (3s/3p) collisions: Differential cross sections, alignment and orientation effects for electron capture, J. Phys. B: At. Mol. Opt. Phys. **26**, 705 (1993).

[38] R. D. Piacentini and A. Salin, Comet hyakutake x-ray source: Charge transfer of solar wind heavy ions, Comput. Phys. Commun. **13**, 57 (1977).

[39] Z. H. Xia, B. Ren, R. T. Zhang, L. Wei, J. Han, T. Meng, J. Wang, P. Ma, Y. Zhang, B. Tu, J. Xiao, K. Yao, Y. Zou, X. L. Zhu, D. L. Guo, X. Ma, and B. Wei, Measurement of *n*- and *l*-resolved state-selective charge exchange in Ar^{8+} collision with He, Astrophys. J. **933**, 207 (2022).

[40] R. K. Janev and H. Winter, State-selective electron capture in atom-highly charged ion collisions, Phys. Rep. **117**, 265 (1985).

[41] S. Otranto, R. E. Olson, and P. Beiersdorfer, X-ray emission cross sections following charge exchange by multiply charged ions of astrophysical interest, Phys. Rev. A **73**, 022723 (2006).

[42] M. Gudmundsson, D. Fischer, N. Haag, H. A. B. Johansson, D. Misra, P. Reinhed, H. Schmidt-Böcking, R. Schuch, M. Schöffler, K. Stöchkel, H. T. Schmidt, and H. Cederquist, Angular scattering in fast ion-atom electron transfer collisions: Projectile wave diffraction and thomas mechanisms, J. Phys. B: At. Mol. Opt. Phys. **43**, 185209 (2010).

[43] H. Agueny, Fraunhofer-type diffraction patterns of matter-wave scattering of projectiles: Electron transfer in energetic ion-atom collisions, Phys. Rev. A **92**, 012702 (2015).

[44] J. W. Gao, Y. Wu, J. G. Wang, N. Sisourat, and A. Dubois, State-selective electron transfer in He^+ + He collisions at intermediate energies, Phys. Rev. A **97**, 052709 (2018).

[45] D. Vernhet, A. Chetioui, K. Wohrer, J. P. Rozet, P. Piquemal, D. Hitz, S. Dousson, A. Salin, and C. Stephan, Alignment of Ne^{8+} n^1P states produced by collisions of Ne^{9+} with H_2 at 4 keV/amu, Phys. Rev. A **32**, 1256 (1985).

[46] S. Schippers, P. Boduch, J. van Buchem, F. W. Bliek, R. Hoekstra, R. Morgenstern, and R. E. Olson, Polarized light emission in keV He^{2+} + Na(3s) collisions, J. Phys. B: At. Mol. Opt. Phys. **28**, 3271 (1995).

[47] L. Liu, Y. Q. Zhao, J. G. Wang, R. K. Janev, and H. Tanuma, Polarization degree differences for the $3p$ $^2P_{3/2} - 3s$ $^2S_{1/2}$ transition of $N^{4+}(3p$ $^2P_{3/2})$ produced in N^{5+}- He and N^{5+}- H_2 collisions, Phys. Rev. A **81**, 014702 (2010).

[48] N. Andersen, J. W. Gallagher, and I. V. Hertel, Collisional alignment and orientation of atomic outer shells I. direct excitation by electron and atom impact, Phys. Rep. **165**, 1 (1988).

[49] J. P. Hansen, L. Kocbach, A. Dubois, and S. E. Nielsen, Orientation and Alignment Effects for Capture in Multiply Charged-ion–atom Collisions, Phys. Rev. Lett. **64**, 2491 (1990).

[50] N. Andersen, J. T. Broad, E. E. Campbell, J. W. Gallagher, and I. V. Hertel, Collisional alignment and orientation of atomic outer shells. II. quasi-molecular excitation, and beyond, Phys. Rep. **278**, 107 (1997).

[51] P. Roncin, C. Adjouri, M. N. Gaboriaud, L. Guillemot, M. Barat, and N. Andersen, Observation of Orientation Propensity for Electron Capture in Multiply-charged-ion–atom Collisions, Phys. Rev. Lett. **65**, 3261 (1990).